Etching of Colloidal InP Nanocrystals with Fluorides: Photochemical Nature of the Process Resulting in High Photoluminescence Efficiency

Dmitri V. Talapin,* Nikolai Gaponik, Holger Borchert, Andrey L. Rogach, Markus Haase, and Horst Weller†

Institute of Physical Chemistry, University of Hamburg, 20146 Hamburg, Germany

Received: June 25, 2002; In Final Form: October 10, 2002

The photoluminescence efficiency of InP nanocrystals prepared via the dehalosilylation reaction between indium chloride and tris-(trimethylsilyl)phosphine in mixtures of trioctylphosphine and trioctylphosphine oxide can be drastically improved by etching with fluorine compounds, as proposed several years ago by Micic et al. A systematic study reported in this communication revealed the pure photochemical nature of this etching process and allowed to improve considerably its reproducibility and reliability. Applying the HF treatment in combination with size-selective photoetching allows to vary the mean size of InP nanocrystals from ∼1.7 nm to 6.5 nm, resulting in monodisperse colloids with band-edge luminescence tunable from green to near-IR and room-temperature quantum yields in the range of 20−40%.

Introduction

Semiconductor nanocrystals with particle sizes of typically less than 10 nm possess a number of unique properties originating from the quantum confinement effect.[1] II−VI nanocrystals were studied extensively during the past two decades, leading to their integration in light-emitting devices[2] and use as biological labels.[3] The information available on and the use of III−V nanocrystals is still much more rare, although there is a strong interest arising from the expectations that the quantum size effects in these materials can be even more pronounced.[4] From the point of view of potential applications, some III−V compounds such as InP are more attractive than the cadmium-containing II−VI semiconductors because of the lower toxicity.

The most reliable colloidal synthesis of InP nanocrystals existing so far is based on Well's dehalosilylation reaction between indium chloride and tris-(trimethylsilyl)phosphine in tri-*n*-octylphosphine oxide (TOPO) or tri-*n*-octylphosphine oxide/tri-*n*-octylphosphine (TOPO/TOP) mixtures.[4−7] As-prepared InP nanocrystals do not possess efficient band edge photoluminescence (PL). A shell of a semiconductor with wider band gap grown around a nanocrystal can drastically enhance the PL efficiency, as has been shown for CdSe nanocrystals with a ZnS shell[8] and for InAs nanocrystals with a CdSe or ZnSe shell.[9] However, in the case of InP, the syntheses of core−shell particles had only a limited success. Thus, growth of $ZnCdS_2$ shells on InP cores yielded nanocrystals with PL efficiency of 5−10%,[10] and growth of ZnS shell followed by aging of the sample for 3 weeks provided the maximal PL efficiency of ∼23%.[11] As an alternative to the core−shell approach, Micic et al. have proposed the post-preparative etching of InP nanocrystals with HF as a way to improve their luminescence efficiency.[12−14] In this communication we show that the etching of InP nanocrystals with fluorine compounds has the photochemical nature, i.e., takes place only under illumination of the colloidal solution. This finding allowed us to improve considerably the reproducibility and reliability of the etching procedure. Applying the nanocrystal surface treatment with HF in combination with the size-selective photoetching technique permits the reproducible preparation of monodisperse fractions of InP nanocrystals whose band edge emission is tunable from green to near-IR with a particle size ranging from ∼1.7 nm to 6.5 nm, and with room-temperature quantum yields in the range of 20−40%.

Experimental Section

The chemicals used were of analytical grade or of the highest purity available. Rhodamin 6G (laser grade, Lambda Physik) and Perylene (Fluka) were used as standards for determining the photoluminescence quantum yields (QY). PL and absorption spectra were measured at room temperature with a FluoroMax-2 spectrofluorimeter (Instruments SA) and a Cary 50 (Varian) UV−vis spectrophotometer, respectively. Powder X-ray diffraction (XRD) spectra were taken on a Philips X'Pert diffractometer. High-resolution transmission electron microscopy (HRTEM) and energy-dispersive X-ray analysis (EDX) were performed on a Philips CM-300 microscope operating at 300 kV.

The TOPO/TOP-stabilized InP nanocrystals were prepared as described in ref 5. Additional injections of precursors ($InCl_3$•TOP and tris-(trimethylsilyl)phosphine) were applied to grow nanocrystals larger than 4.5 nm. The crude solutions were subjected to size-selective precipitation[4] using toluene and methanol as solvent and nonsolvent, respectively, to isolate nearly monodisperse nanocrystal fractions which were subsequently redispersed in hexane. Absorption spectra, TEM and HRTEM images of size-selected InP nanocrystals are shown in the Supporting Information. The concentration of InP nanocrystals in each size-selected fraction was estimated from the absorption spectrum using values of the molar extinction coefficient of InP nanocrystals of different size (Table 1).[15] Briefly, the extinction coefficients were estimated by digesting the nanocrystals in HNO_3 and measuring the total indium concentration by ICP mass-spectroscopy analysis.

* Corresponding author. Fax: +49-40-42838-3452. E-mail: talapin@chemie.uni-hamburg.de

† Homepage: http://www.chemie.uni-hamburg.de/pc/AKs/Weller/

10.1021/jp026380n CCC: $22.00
Published on Web 11/14/2002

TABLE 1: Size Dependent Molar Extinction Coefficients of InP Nanocrystals

particle size, nm	molar extinction coefficient at 350 nm,[a] 1/(mol cm)
2.8	7.2×10^5
3.4	1.3×10^6
3.9	2.5×10^6
4.2	3.1×10^6
4.5	3.6×10^6
4.8	4.3×10^6
5.2	5.2×10^6

[a] We used the values of the molar extinction coefficient estimated far from the absorption onset to minimize the error coming from finite particle size distribution.

The etching of the InP nanocrystals with HF was typically performed in air as follows. An aliquot of InP nanocrystals containing $\sim 1 \times 10^{-7}$ mol of particles dispersed in hexane was mixed with 25 mL of *n*-butanol and 0.25 g of TOPO (Merck, 98%) was added. InP nanocrystals larger than ~5 nm are insoluble in *n*-butanol, therefore isooctane (5−20 mL) was added to the etching solution until it became optically clear. The mixture was loaded into a 50 mL vessel from transparent perfluoroethylene, and 25−200 μL of HF-containing etching solution was added under stirring. The HF-etching solution was prepared by mixing 0.527 mL of aqueous HF (40 wt. % solution), 0.065 mL of H_2O, and 5.0 mL of *n*-butanol. In the photochemical etching experiments, the reaction mixture was illuminated by light from a 450 W xenon lamp passed through a long pass filter with the cutoff wavelength depending on the particle size. The process of etching was finished in ~15 h. The etched nanocrystals were isolated from the reaction mixture by addition of 25 mL of acetonitrile, centrifugation of the suspension of flocculated nanocrystals, and subsequent redispersion of them in hexane or another nonpolar solvent. Isolated InP nanocrystals were stable both under nitrogen and in air and retain their photoluminescence efficiency over weeks.

A number of other fluorine compounds were additionally tested as etching agents for InP nanocrystals. Luminescence efficiencies comparable with that observed after treatment with HF (20−40%) were achieved with NH_4F, $N(C_4H_9)_4F \cdot 3H_2O$, pyridine poly(hydrogen fluorine), and HF-melamine complexes. The use of KF·[18-crown-6] complex and hexadecylamine hydrofluoride resulted in luminescence efficiencies of about 3−5%, and *n*-hexylfluoride did not improve the emission of InP nanocrystals at all.

The etching procedure required an excess of the stabilizing agent (TOPO), as will be discussed below. The use of dodecanethiol instead of TOPO resulted in similar luminescent properties, whereas primary amines (e.g., hexadecylamine) yielded lower PL efficiencies. In the case of large InP nanocrystals poorly soluble in butanol, the two-phase etching approach where InP nanocrystals were dissolved in one phase (isooctane) and HF was dissolved in another phase (acetonitrile), as described in ref 14, provided better results. In the case of small InP nanocrystals the one-phase (butanol) and two-phase (isooctane/acetonitrile) procedures could be used equally effectively.

Results and Discussion

Figure 1 shows the evolution of the absorption and the PL spectra of InP nanocrystals after the addition of different amounts of HF. When the HF treatment of InP nanocrystals was performed in darkness, the band edge PL enhanced by more than 1 order of magnitude and minor changes in the absorption spectra were observed (Figures 1a,b). However, the resulting

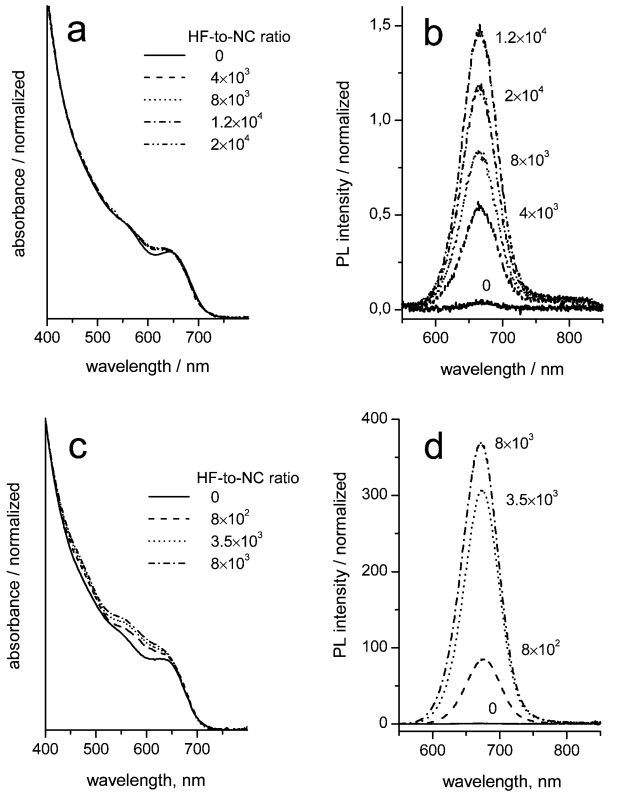

Figure 1. Evolution of absorption (a, c) and PL (b, d) spectra upon the treatment of InP nanocrystals with different amounts of HF in the darkness (a, b) and under illumination of the etching solution with the light of a 450 W xenon lamp passed through the long pass filter with cutoff at 610 nm (c, d). The numbers show the ratio of initial concentration of HF molecules to InP nanocrystals in the etching mixture.

PL QY was still low and did not exceed 0.1−0.3%. Further increase of the initial concentration of HF resulted in a decrease of the PL efficiency as seen in Figure 1b. Etching under anaerobic conditions (i.e., under nitrogen) provides the same results as etching in air. This behavior was observed for all fractions of InP nanocrystals, independent of their size.

However, we found that the samples etched under occasional illumination of colloidal solution with daylight exhibited higher PL efficiencies. Therefore, in a second series of experiments, the etching was performed under illumination with photons having an energy above the band gap energy of InP nanocrystals. The PL efficiency of the samples etched under illumination increased drastically (by more than 3 orders of magnitude), reaching values of 20−40%. Figures 1c,d show how the resulting absorption and PL spectra depend on the initial ratio between InP nanocrystals and HF molecules. In fact, a correlation between the PL efficiency and the etching-induced features in the absorption spectrum was observed (Figure 1c).

Figure 2a summarizes the above findings. Combination of the HF treatment with illumination resulted in a drastic increase of the band edge PL achieving the room-temperature QY as high as 20−40%. In contrast, the long term (days) treatment of InP nanocrystals with HF at room temperature in darkness enhances the PL efficiency to the maximum of ~0.3% QY only. The same behavior was observed when the reaction mixture was heated to 40−50°C showing that heating of the sample by absorption of IR irradiation cannot be responsible for the luminescence improvement under illumination. Illumination of InP nanocrystals in the absence of HF did not result in considerable improvement of the PL efficiency.

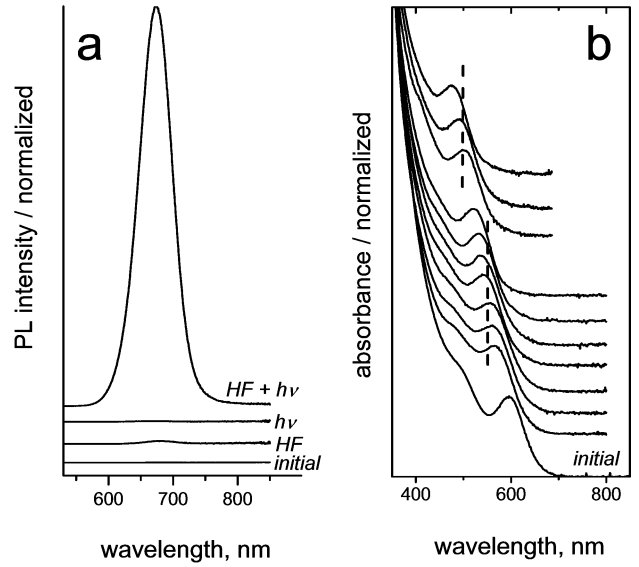

Figure 2. (a) Representative PL spectra measured for InP nanocrystals of the same size before treatment with HF (initial), after treatment with HF (24 h, $\sim 3.5 \times 10^3$ HF molecules per one InP particle), after illumination in the absence of HF ($h\nu$), and after illumination in the presence of $\sim 3.5 \times 10^3$ HF molecules per one InP particle (HF+$h\nu$). (b) Evolution of absorption spectra during size-selective photoetching of small InP nanocrystals. The vertical dashed lines show the cutoff wavelength of the long pass filter.

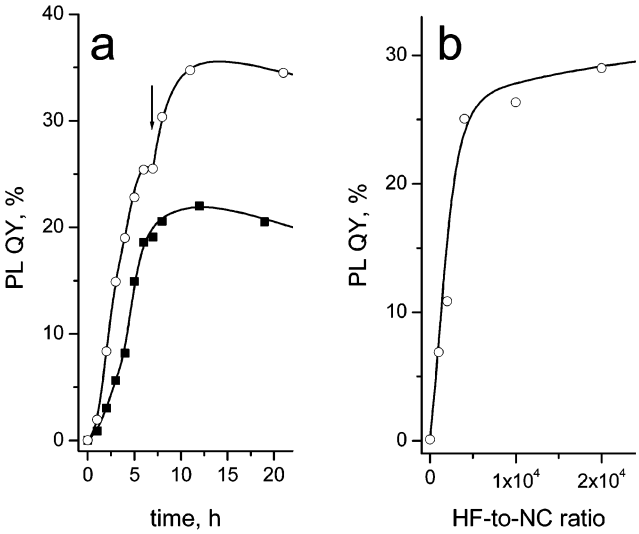

Figure 3. (a) Temporal evolution of the PL QY during photoetching of 4.5 nm (■, PL_{max} 700 nm, $\sim 6 \times 10^3$ HF molecules per one particle) and 3 nm (○, PL_{max} 630 nm, $\sim 3 \times 10^3 + 1.5 \times 10^3$ HF molecules per one particle) InP nanocrystals. The arrow shows the additional injection of HF etching solution. (b) Dependence of the resulting PL QY after 15 h of photoetching of 4 nm InP nanocrystals on the initial amount of HF.

The temporal evolution of the PL efficiency of InP nanocrystals upon treatment with HF under illumination was monitored by measuring the PL spectra of aliquots taken from the reaction mixture at different instants of time (Figure 3a). As a rule, the highest PL QY was achieved when the etching was performed for 10 h or more, even at high illumination intensities. The PL efficiency reached a certain level and then slowly decayed. The maximum value of the resulting PL QY varied slightly from sample to sample, even when these samples were isolated from the same aliquot of the crude solution by size-selective precipitation. This might be a result of different initial surface roughness observed for different nanocrystal fractions in the crude solution and originating from the Ostwald ripening growth mechanism.[16] The nanocrystals with smoother surface provide higher resulting PL efficiencies and require less HF for their successful etching.

The PL efficiency achieved after treatment of InP nanocrystals with different amounts of HF under the same illumination conditions is presented in Figure 3b. In the case of ~4 nm large InP nanocrystals, the PL QY reaches the saturation level after addition of about $\sim 5 \times 10^3$ HF molecules per InP particle. Addition of the required amount of HF in several steps resulted in a higher final PL efficiency (Figure 3a, additional HF injection indicated by arrow).

The etching of InP nanocrystals with HF results in a slight decrease of their size.[5,12−14] In the case of "large" (>~4 nm) InP nanocrystals, the etching is accompanied by a small blue shift (5−10 nm) of the PL maximum (Figure 1d). Smaller nanocrystals exhibit a larger blue shift of the emission band during the etching process. In principle, it is possible to control this decrease of the particle size by progressive addition of HF, since this results in slow dissolution of the nanocrystals, whereas the final value of the PL QY remains nearly constant. However, according to the literature data[4] and our experiments, the etching rate (in terms of relative decrease of the nanocrystal size per time unit) strongly increases with decreasing InP nanocrystal size, thus leading to substantial broadening of the particle size distribution in the course of etching. As the spectral width, or the "color purity" of the nanocrystal emission, is proportional to the width of the particle size distribution, it is difficult to obtain highly luminescent InP nanocrystals with narrow band edge emission during the etching under white light, i.e., under conditions where particles of all sizes were excited. Taking into account the photochemical nature of the etching process, we have solved this dilemma by combining the HF treatment with the so-called size-selective photoetching technique. The last approach utilizes the quantum confinement effect, in particular the dependence of the absorption edge of semiconductor nanoparticles on their size.[17−19] As the absorption onset of smaller particles is shifted toward blue with respect to that of larger particles, the illumination of colloidal solution through a suitable long pass filter results in a situation where only the largest particles in a given ensemble are excited; whereas the smallest are not. Upon etching, the size of the excited particles decreases until the absorption onset shifts into the wavelength region blocked by the filter and the photochemical etching of these particles terminates.

The application of size-selective photoetching in combination with the progressive addition of HF results in controllable decrease of the mean particle size, as evidenced from the blue shift of the absorption spectrum (Figure 2b). The size distribution of InP nanocrystals keeps narrow at all stages of etching, including the very late stages, as is seen from the quality of absorption spectra presented in Figures 2b and 4a. The width of the final particle size distribution was dictated mainly by the characteristics of the cutoff filter used. It was possible to obtain highly luminescent fractions of extremely small InP nanocrystals with diameters considerably below 2 nm (absorption maximum below 500 nm, green emission) with relatively narrow size distribution. To the best of our knowledge, preparation of such small InP nanocrystals with high band edge PL has not been achieved by any other approach. To prepare nanocrystals emitting in a desired spectral region, we also varied the initial size of InP nanocrystals. In combination with the size-selective photoetching technique, this allowed tuning the emission wavelength precisely in the wide spectral region. For

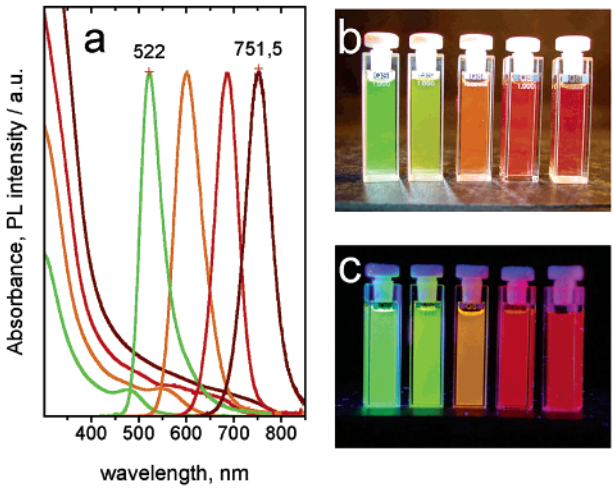

Figure 4. (a) Absorption and PL spectra of HF-photoetched InP nanocrystals of different size. (b, c) Visualization of size-dependent change of the photoluminescence color of HF-photoetched InP nanocrystals. The smallest (~1.7 nm) particles emit green, whereas ~4 nm particles emit deep red. Larger InP nanocrystals emit in near-IR (not shown). The high PL quantum yield makes the colloidal solutions "glow" in room light (b). Photo (c) shows the luminescence of the etched InP nanocrystals placed under UV-lamp.

instance, etching of the largest (~6.5 nm diameter) InP nanocrystals yields nanocrystals emitting in the near-IR with a PL maximum at ~760 nm. A set of absorption and PL spectra of photochemically etched InP nanocrystals of different size is shown in Figure 4a, together with the photographs of the luminescent colloidal solutions (Figures 4b and 4c). The absorption spectra of InP nanocrystals larger than ~4 nm look rather smooth and featureless (e.g., Figure 4a, red and brown curves) even when narrow PL bands and TEM images manifest fairly narrow size distributions of the etched InP nanocrystals (Figure S3, Supporting Information). The PL excitation spectra (Figure S4, Supporting Information) show that the absorption edge of "large" InP nanocrystals consists of several overlapping transitions with similar intensities. As already mentioned above, the room temperature PL QY of the etched samples was typically in the range between 20 and 40% for all particle sizes. Some nanocrystal fractions had PL efficiencies above 40%, indicating the possibility of further improvement of the luminescent properties of InP nanocrystals through optimization of the etching conditions.

The InP nanocrystals can be isolated from the etching mixture by precipitating them with acetonitrile and subsequent redispersion in a desired nonpolar organic solvent. TEM and HRTEM images of the etched InP nanocrystals show that the nanocrystals retain their spherical shape, monodispersity, and crystallinity (Figure S3, Supporting Information). EDX measurements indicate the presence of a small amount of fluorine in the etched nanocrystals.

The stability of luminescent properties of the etched InP nanocrystals is a parameter being crucially important for their potential applications. The PL intensity of the photoetched InP nanocrystals dispersed in toluene or butanol was found to be rather stable, although it moderately decreased when the samples were stored under daylight. The smallest (<2 nm) and the largest (>5 nm) InP nanocrystals exhibited lower PL stability compared to the particles of the middle sizes. The highest stability was observed for red-emitting particles 3.5−4 nm in diameter. It was also found that both the long-term stability and photostability of the PL efficiency of the photoetched InP nanocrystals of any size considerably increases if some additional amount of TOPO (1−2 wt %) is added to the colloidal solution. This observation allows us to consider the importance of the equilibrium between the TOPO molecules coordinating the particle surface and the excess of TOPO molecules in solution. The presence of additional TOPO in solution promotes the formation of a complete protective TOPO shell around the nanocrystals, preventing degradation of their luminescent properties. Summarizing, the stability of properties and processability of the photoetched InP nanocrystals was found to be comparable to that of TOPO-capped CdSe nanocrystals, which allows considering them as a promising material for various applications.

The photochemical nature of the InP nanocrystal etching requires a revision of the conventional description of the etching mechanism. According to Micic et al., etching with HF removes surface phosphorus vacancies serving as electron traps.[12] On the other hand, the photochemical nature of the etching provides evidence that photogenerated carriers play a dominant role. In the case of bulk *n*-InP, the rate-limiting step of the photoetching process is the capture of the photogenerated hole by the phosphorus surface dangling bond, activating it for an attack with a fluorine ion from solution.[20,21] The hole surface states were recently detected on InP nanocrystals using EPR[22] technique. Probably these surface hole traps are associated with the P-dangling bonds and elimination of these traps upon etching in combination with the filling of the phosphorus vacancies by fluorine results in the strong enhancement of the band edge PL. A more detailed study of the mechanism of InP photochemical etching is currently underway.

Acknowledgment. We thank Andreas Kornowski and Sylvia Bartholdi-Nawrath for TEM and HRTEM investigations. Special appreciation goes to the colleagues from HASYLAB/DESY, Sorin Adam, and Dr. Colm McGinley for XPS investigations and useful discussions. This work was supported by the BMBF, Philips, and by the Deutsche Forschungsgemeinschaft through the SFB 508.

Supporting Information Available: Absorption and photoluminescence excitation spectra, TEM, and HRTEM images of size-selected fractions of InP nanocrystals before and after the photoetching with HF. This material is available free of charge via the Internet at http://pubs.acs.org.

References and Notes

(1) For reviews see, e.g.,: Brus, L. E. *Appl. Phys. A* **1991**, *53*, 465. Wang, Y.; Herron, N. J. *Phys. Chem.* **1991**, *95*, 525. Banyai, L.; Koch, S. W. *Semiconductor Quantum Dots*, World Scientific: Singapore, 1993. Weller, H. *Angew. Chem., Int. Ed. Engl.* **1993**, *32*, 41. Weller, H. *Adv. Mater.* **1993**, *5*, 88. Alivisatos, A. P. *J. Phys. Chem.* **1996**, *100*, 13226. Woggon, U. *Optical Properties of Semiconductor Quantum Dots*; Springer-Verlag: Berlin, 1997. Gaponenko, S. V. *Optical Properties of Semiconductor Nanocrystals;* Cambridge University Press: Cambridge, 1998.

(2) Colvin, V. L.; Schlamp, M. C.; Alivisatos, A. P. *Nature* **1994**, *370*, 354.

(3) Bruchez, M. P.; Moronne, M.; Gin, P.; Weiss, S.; Alivisatos, A. P. *Science* **1998**, *281*, 2013.

(4) Guzelian, A. A.; Katari, J. E. B.; Kadavanich, A. V.; Banin, U.; Hamad, K.; Juban, E.; Alivisatos, A. P.; Wolters, R. H.; Arnold, C. C.; Heath, J. R. *J. Phys. Chem.* **1996**, *100*, 7212.

(5) Micic, O. I.; Nozik, A. J. *Handbook of Nanostructured Materials and Nanotechnology*, Nalwa, H. S., Ed.; Academic Press: San Diego, 2000; v. 1, 427.

(6) Micic, O. I.; Curtis, C. J.; Jones, K. M.; Sprague, J. R.; Nozik, A. J. *J. Phys. Chem.* **1994**, *98*, 4966.

(7) Micic, O. I.; Sprague, J. R.; Curtis, C. J.; Jones, K. M.; Machol, J. L.; Nozik, A. J.; Giessen, H.; Fluegel, B.; Mohs, G.; Peyghambarian, N. *J. Phys. Chem.* **1995**, *99*, 7754.

(8) Hines, M. A.; Guyot-Sionnest, P. *J. Phys. Chem.* **1996**, *100*, 468.

(9) Cao, Y. W.; Banin, U. *J. Am. Chem. Soc.* **2000**, *122*, 9692.
(10) Micic, O. I.; Smith, B. B.; Nozik, A. J. *J. Phys. Chem. B* **2000**, *104*, 12149.
(11) Haubold, S.; Haase, M.; Kornowski, A.; Weller, H. *ChemPhysChem.* **2001**, *2*, 331.
(12) Micic, O. I.; Sprague, J.; Li, Z.; Nozik, A. J. *Appl. Phys. Lett.* **1996**, *68*, 3150.
(13) Micic, O. I.; Cheong. H. Fu; Zunger, A.; Sprague, J. R.; Mascarenhas, A.; Nozik, A. J. *J. Phys. Chem. B* **1997**, *101*, 4904.
(14) Micic, O. I.; Jones, K. M.; Cahill, A.; Nozik, A. J. *J. Phys. Chem. B* **1998**, *102*, 9791.
(15) Talapin, D. V. PhD Thesis *Experimental and theoretical studies on the formation of highly luminescent II−VI, III−V and core−shell semiconductor nanocrystals*", University of Hamburg, Hamburg, Germany 2002. http://www.chemie.uni-hamburg.de/bibliothek/diss2002.html.
(16) Talapin, D. V.; Rogach, A. L.; Shevchenko, E. V.; Kornowski, A.; Haase, M.; Weller H. *J. Am. Chem. Soc.* **2002**, *124*, 5782.
(17) Dijken, A.; Vanmaekelbergh, D.; Meijerink, A. *Chem. Phys. Lett.* **1997**, *269*, 494.
(18) Dijken, A.; Janssen A. H.; Smitsmans, M. H. P.; Vanmaekelbergh, D.; Meijerink, A. *Chem. Mater.* **1998**, *10*, 3513.
(19) Torimoto, T.; Kontani, H.; Shibutani, Y.; Kuwabata S.; Sakata, T.; Mori, H.; Yoneyama, H. *J. Phys. Chem. B* **2001**, *105*, 6838.
(20) Hens, Z.; Gomes, W. P. *J. Phys. Chem. B* **2000**, *104*, 7725.
(21) Erne, B. H.; Vanmaekelbergh, D.; Vermeir, I. E. *Elechtrochim. Acta* **1993**, *38*, 2259.
(22) Micic, O. I.; Nozik, A. J.; Lifshitz, E.; Rajh, T.; Poluektov, O. G.; Thurnauer, M. C. *J. Phys. Chem. B* **2002**, *106*, 4390.